

Bridging the Gap: A Unified Video Comprehension Framework for Moment Retrieval and Highlight Detection

Yicheng Xiao^{1*}, Zhuoyan Luo^{1*}

Yong Liu¹, Yue Ma¹, Hengwei Bian², Yatai Ji¹, Yujiu Yang^{1†}, Xiu Li^{1†}

¹Tsinghua Shenzhen International Graduate School, Tsinghua University

²Carnegie Mellon University

{xiaoyc23, luozy23}@mails.tsinghua.edu.cn

Abstract

Video Moment Retrieval (MR) and Highlight Detection (HD) have attracted significant attention due to the growing demand for video analysis. Recent approaches treat MR and HD as similar video grounding problems and address them together with transformer-based architecture. However, we observe that the emphasis of MR and HD differs, with one necessitating the perception of local relationships and the other prioritizing the understanding of global contexts. Consequently, the lack of task-specific design will inevitably lead to limitations in associating the intrinsic specialty of two tasks. To tackle the issue, we propose a Unified Video COMprehension framework (UVCOM) to bridge the gap and jointly solve MR and HD effectively. By performing progressive integration on intra and inter-modality across multi-granularity, UVCOM achieves the comprehensive understanding in processing a video. Moreover, we present multi-aspect contrastive learning to consolidate the local relation modeling and global knowledge accumulation via well aligned multi-modal space. Extensive experiments on QVHighlights, Charades-STA, TACoS, YouTube Highlights and TVSum datasets demonstrate the effectiveness and rationality of UVCOM which outperforms the state-of-the-art methods by a remarkable margin. Code is available at <https://github.com/EasonXiao-888/UVCOM>

1. Introduction

Video has emerged as a highly favored multi-medium format on the internet with its diverse content. This significant surge in online video encourages users to adjust their strategies for accessing desired video contents. Instead of spending time-consuming efforts inspecting the whole video, they are more inclined to directly obtain particular clips of interest through language descriptions. This

*Equal contribution. † Corresponding author.

Query: A video collection of wonderful places to visit

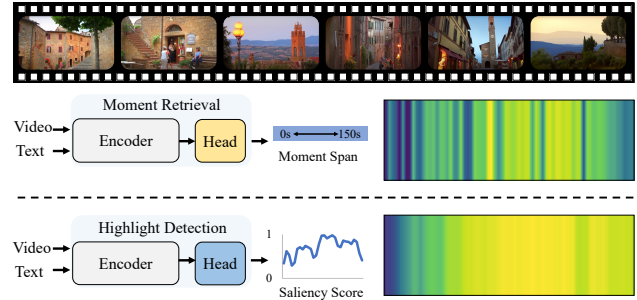


Figure 1. **Illustration of the intrinsic characteristics of Moment Retrieval and Highlight Detection.** We visualize the attention map of the same video under two tasks. The attention map for MR takes on strip-like patterns, indicating the emphasis of local relationships. In contrast, it is in band-like format for HD, which signifies the focus on global information.

shift in user preference gives rise to two significant research topics: Video Moment Retrieval [8, 23, 35, 52, 53], focuses on locating the specific moment, and Highlight Detection [1, 11, 45, 48, 50], is dedicated to identifying segments of high saliency.

Actually, it is apparent that two tasks share many common characteristics, *e.g.*, identifying relevant video segments in response to textual expressions. In light of the above, Lei *et.al.* [18] first proposes a novel dataset named QVHighlights and a basic framework called Moment-DETR to jointly solve both tasks. UMT [24] incorporates extra audio modality and QD-DETR [26] produces text-query dependent video representation to achieve better performance. The above-mentioned methods simply model MR and HD as a multi-task problem and mainly concentrate on utilizing non-specific strategy to solve them. In particular, they all adopt a straightforward way to train and optimize both tasks together with general design, *e.g.*, transformer-based models. However, we revisit the characteristics of MR/HD and discover that there exists a gap be-

tween them as illustrated in Fig. 1. which leads to the challenge in consistent performance on both tasks, *i.e.*, achieving precise moment localization and accurate highlight-ness estimation simultaneously.

Therefore, we consider that the design of framework should follow two principles to alleviate the above weakness: 1) **Local Relation Activation**: MR necessitates the understanding of local relationships within the video to accurately localize specific segments. 2) **Global Knowledge Accumulation**: The objective of HD is to fit the saliency distribution of the entire video, emphasizing the importance of global context (in Fig. 1). Based on the principles, we propose a Unified Video Comprehension Framework (UVCOM) to seamlessly integrate the emphasis of MR and HD, which effectively bridges the gap and achieves great performance on both tasks consistently. Specifically, we first design a novel Comprehensive Integration Module (CIM) to progressively facilitate the integration on intra and inter-modality across multi-granularity. CIM first efforts to propagate the aggregated semantic phrases from the text into the visual feature to realize local relationship perception. Then, it accumulates global information from video by utilizing the moment-awareness feature as an intermediary. With a comprehensive view of the entire video, CIM facilitates the understanding of particular intervals and highlight contents, which is beneficial to identify the desired moment and non-related ones. Furthermore, we introduce a multi-aspect contrastive learning which incorporates clip-text alignment to consolidate the local relation modeling, and video-linguistic discrimination to enhance the quality of accumulated global information.

We conduct extensive experiments on five popular MR/HD benchmarks to validate the effectiveness of our framework and the results show that UVCOM notably outperforms existing methods for all benchmarks.

Overall, our contributions are summarized as follows:

- Based on our investigation into the emphasis of Moment Retrieval and Highlight Detection, we present two principles for framework design. Guided by them, we propose a Unified Video Comprehension Framework called UVCOM to effectively bridge the gap between two tasks.
- In UVCOM, a Comprehensive Integration Module (CIM) is designed to perform progressive intra and inter-modality interaction across multi-granularity, which achieves locality perception of temporal and multi-modal relationships as well as global knowledge accumulation of the entire video.
- Without bells and whistles, our method outperforms all existing state-of-the-art methods by a remarkable margin, *e.g.*, +5.97% in R1@0.7 for MR than UniVTG [21] on TACoS [32] and +3.31% in HIT@1 for HD than QD-DETR [26] on QVHighlights [18].

2. Related Work

Moment Retrieval. Moment Retrieval is a task that aims at retrieving the target moment, *i.e.*, one [8] or many [17] continuous intervals in a video given the text description. Generally, the model will focus more on the relationship across adjacent frames for better localization. Previous works retrieve video intervals into two perspectives: proposal-based and proposal-free. The proposal-based methods [8, 12, 39, 44] follow the propose-then-rank pipeline, where they first generate candidate proposals then rank them based on matching scores. Liu *et al.* [22] and Hendricks *et al.* [12] utilize sliding windows to scan the entire video for candidate proposals generation and calculate the similarity with textual embedding for selection. To enhance temporal awareness, MAN [53] and Gao *et al.* [9] both introduce graph convolution network to capture temporal dependency across adjacent moments. On the other hand, the proposal-free methods [19, 27, 29, 40, 51, 54] directly regress the start and end timestamp via video-text interaction. Yuan *et al.* [51] and Mun *et al.* [27] generate the temporal coordinates of sentence by multi-modal co-attention mechanism. Furthermore, Rodriguez *et al.* [29] utilizes a simple dynamic filter instead of cross attention to match video and text embedding.

Highlight Detection. Highlight Detection aims to identify highlights or important segments with high potential appeal in a video. Compared with Moment Retrieval, It is necessary for the model to associate the whole video content for fitting saliency distribution of each clip. Many prior works [11, 45, 48, 48, 50] adopt ranking formulation where they rank the important segments with higher score. Video2Gif [11] trains a generic highlight predictor to produce GIF from videos. Rochan *et al.* [34] designs a task-specific highlight detectors to automatically create highlights from the user history. They all use the fine-grained annotations for training which are labor-intensive and expensive. Therefore, Xiong *et al.* [45] proposes to learn highlights only with video-level label. Recently, Badamdorj *et al.* [1] elaborates on fusing visual and audio content to generate better video representations.

MR and HD share many similar properties. Moment-DETR [18] puts forward a novel dataset which first includes two tasks and provides a simple DETR-based [2] network. To improve the query quality, UMT [24] proposes to adopt audio, visual and text content for query generation. Furthermore, QD-DETR [26] exploits the textual information by involving video-text pair negative relationship learning, achieving greater performance. However, previous methods simply train and optimize two tasks without considering the different emphasis of each task. To address this issue, we propose a novel unified framework UVCOM that effectively associates the speciality of MR and HD to achieve

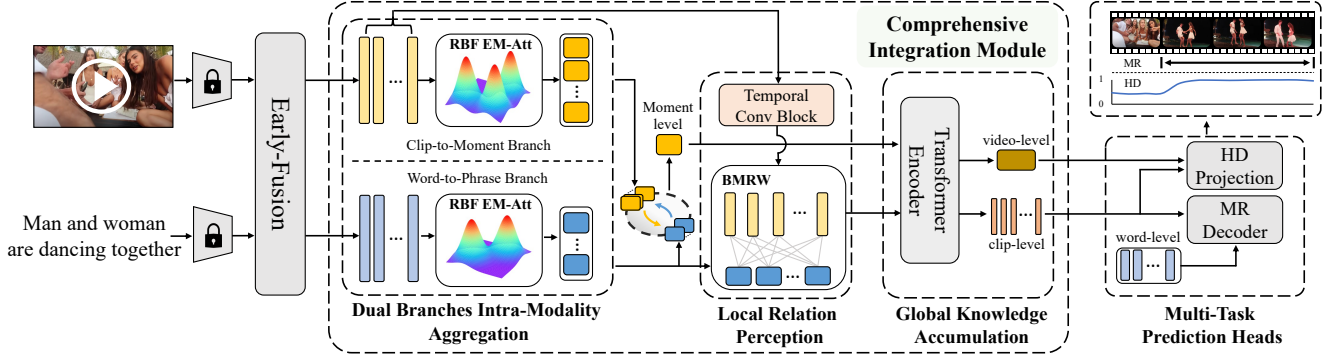


Figure 2. **Overview of UVCOM.** Based on the exploration of MR and HD, we propose a unified video comprehension framework guided by the design principles. Specifically, the model takes a video with language description as input. After encoding and early-fusion process, we design a Comprehensive Integration Module (CIM) to achieve subsequent progressive integration on intra and inter-modality across multi-granularity. Finally, the multi-task heads output the moment spans for MR and saliency scores for HD.

comprehensive understanding.

3. Method

Given a video of L clips $\{v_1, v_2, \dots, v_l\}$ and a textual expression of N words $\{e_1, e_2, \dots, e_n\}$, the goal of MR is to localize the most relevant moment with the center coordinate and duration, while HL is to generate the saliency score distribution for the whole video.

3.1. Visual-Text Encoding

Visual Encoder. Following previous works [18, 21, 24, 26], we utilize the pretrained backbone, *e.g.*, SlowFast [6], video encoder of CLIP [31] and I3D [3] to extract visual features $\mathcal{F}_v \in \mathbb{R}^{L \times D}$ of the video. Note that D demotes the channel.

Language Encoder. Simultaneously, text encoder of CLIP is adopted to encode the linguistic expression into the textual embedding $\mathcal{F}_t \in \mathbb{R}^{N \times D}$.

With the visual and textual features, we apply a bidirectional transformer-based encoder to perform the early fusion. It coarsely encodes features in different modalities and outputs preliminary aligned visual and textual representations.

3.2. Comprehensive Integration Module

After getting the visual and textual representations, we design a Comprehensive Integration Module (CIM) to perform progressive intra and inter-modality integration across multi-granularity. Specifically, we leverage Expectation-Maximum (EM) Attention [20] on associating inner-modality content to generate the moment-wise visual features and phrase-wise textual features, respectively. Then we propose Local Relation Perception (LRP) module to unify temporal relationship modeling and inter-modality fusion, which reformulates the temporal and modality inter-connection to enhance the locality perception. Finally, we

utilize a standard encoder to produce the video-wise feature by integrating the correlation between moment and clip-wise visual features.

Dual Branches Intra-Modality Aggregation. A video usually contains more than one event and irrelevant background scenes. The same scenario happens in textual descriptions where insignificant words and unconstrained expressions may cause potential ambiguity. To tackle the problem, we propose to utilize RBF-kernel based EM Attention [14, 20] to aggregate the clip/word-level features. As shown in Fig. 2, it is a dual-branches structure. The clip-to-moment branch aims at incorporating the relationship of each clip to enhance the desired event representations while suppressing the background noise. Meanwhile, the word-to-phrase branch is to emphasize the referred moment description by accumulating contextual information.

Specifically, we fit the distribution of \mathcal{F}_v and \mathcal{F}_t by a separated Gaussian Mixture Model [33] to generate the compact moment and phrase-level representations via the centroid of Gaussians. Taking \mathcal{F}_v as an example, we utilize a linear superposition of n_v Gaussians to capture the statistics of $f_v^i \in \mathbb{R}^D$ (the i -th snippet of \mathcal{F}_v):

$$p(f_v^i) = \sum_{k=1}^{n_v} z_k^v \mathcal{N}(f_v^i | \mu_k, \Sigma_k), \quad (1)$$

where $z_k^v \in \mathbb{R}$, $\mu_k \in \mathbb{R}^D$ and $\Sigma_k \in \mathbb{R}^{D \times D}$ denote the weight, mean and covariance of k -th Gaussian basis for the clip-to-moment branch. We substitute the covariance with an identity matrix I for simplification and employ the radial basis function (RBF Kernel) $\mathcal{K}(f_v^i, \mu_k)$ to estimate the posterior probability $\mathcal{N}(f_v^i | \mu_k, \mathcal{I})$:

$$\mathcal{K}(f_v^i, \mu_k) = \exp(-\lambda \|f_v^i - \mu_k\|_2^2), \quad (2)$$

where $\lambda > 0$ is an adjustable hyper-parameter to control the distribution. Afterwards, at t -th iteration, we update the

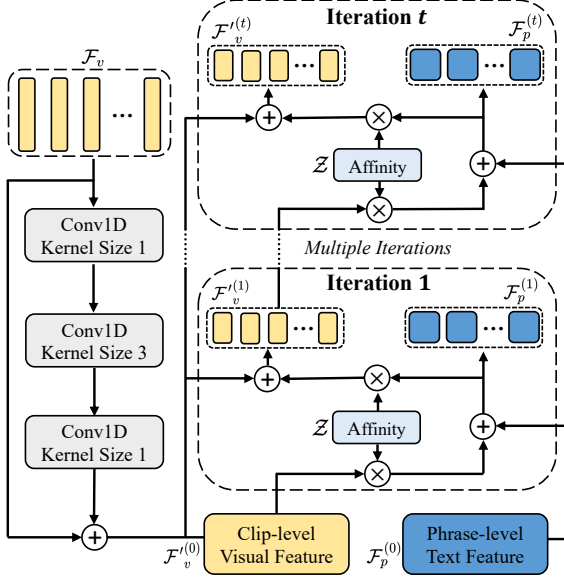


Figure 3. **Illustration of Local Relation Perception (LRP) module.** We first process the visual feature \mathcal{F}_v with a Conv1D Block. Then we develop a Bidirectional Modality Random Walk (BMRW) algorithm to exploit the power of fine-grained multi-modal interaction. The affinity \mathcal{Z} is generated by scaled dot product: $\mathcal{Z} = \lambda_z \mathcal{F}_v^{(0)} (\mathcal{F}_p^{(0)})^\top$.

weight $Z^{(t)} \in \mathbb{R}^{L \times n_v}$ in the E Step and re-estimate $\mu^{(t)} \in \mathbb{R}^{n_v \times D}$ in the M step, which can be formulated as:

$$\mu^{(t)} = \text{Norm}_1(Z^{(t)})^T F_v, \quad t \in \{1, \dots, T\}. \quad (3)$$

Furthermore, in contrast to conventional cluster methods that only involve iterative update, the initialized means $\mu^{(0)}$ we set are learnable. Therefore, they can effectively capture the feature distribution of the dataset through the standard back-propagation.

After t iterations, we obtain the fine-grained moment-wise representation \mathcal{F}_m from $\mu^{(t)}$ which fully aggregates the contextual information. Similarly, we operate the above steps on word-to-phrase branch to generate the phrase-level linguistic feature $\mathcal{F}_p \in \mathbb{R}^{n_t \times D}$, where n_t indicates the number of Gaussian basis in word-to-phrase branch.

Local Relation Perception. Previous methods [18, 24, 26] directly perform cross-modal fusion between clip and word-level features, disregarding the temporal relation and valuable semantic interaction across different granularities. Without the information from adjacent clips, the simple and coarse clip-word fusion will easily deviate the model from focusing on the relevant boundary clips, causing incorrect localization. To address the aforementioned weakness, we design a Local Relation Perception (LRP) module to excavate both temporal and inter-modality relationships. As shown in Fig. 2, we first utilize a temporal convolution block to improve the locality perception of clip-level fea-

tures, which can be formulated as:

$$\mathcal{F}'_v = \text{Conv}(\mathcal{F}_v) + \mathcal{F}_v. \quad (4)$$

Since simply incorporate clip-level relation may introduce local redundancy, we leverage fine-grained inter-modal interaction to re-calibrate the attention for activating the relevant moments. Intuitively, a straightforward approach is to utilize cross-attentive mechanism [24, 26] to perform inter-modal interaction. Nevertheless, the complex scenario in an untrimmed video, *e.g.*, footage transitions and irrelevant events, will increase the likelihood of attention drift which leads to the undesirable local activation. Moreover, although phrase-wise linguistic features specify referred moment description and alleviate the impact of noise in contrast to word-wise one, it may potentially contribute to attention drift due to the irrelevant accumulated words. Therefore, inspired by [10, 14, 28], we design a bidirectional modality random walk (BMRW) algorithm to mitigate the mentioned drawbacks and fully exploit the power of the fine-grained multi-modal interaction. It propagates the textual prior into the visual features for highlighting the corresponding local context and suppressing unrelated ones. Simultaneously, linguistic features are refined through the incorporation of updated visual content. As shown in Fig. 3, there are multiple iterations in BMRW where two modalities features learn collaboratively in visual-linguistic shared embedding space until convergence.

Formally, we first define the $\mathcal{F}'_v, \mathcal{F}_p$ as initial features $\mathcal{F}'_v^{(0)}, \mathcal{F}_p^{(0)}$ at 0-th iteration and formulate affinity \mathcal{Z} by scaled dot product: $\mathcal{Z} = \lambda_z \mathcal{F}'_v^{(0)} (\mathcal{F}_p^{(0)})^\top$, where λ_z is the scaling factor. At t -th iteration, the phrase-wise linguistic feature $\mathcal{F}_p^{(t)}$ is updated by the original feature $\mathcal{F}_p^{(0)}$ and the visual output $\mathcal{F}'_v^{(t-1)}$ from previous iteration:

$$\mathcal{F}_p^{(t)} = \omega \text{Norm}_1(\mathcal{Z})^\top \mathcal{F}'_v^{(t-1)} + (1 - \omega) \mathcal{F}_p^{(0)}, \quad (5)$$

Subsequently, it is projected into the temporal-awareness feature $\mathcal{F}'_v^{(t)}$:

$$\mathcal{F}'_v^{(t)} = \omega \mathcal{Z} \mathcal{F}_p^{(t)} + (1 - \omega) \mathcal{F}'_v^{(0)}, \quad (6)$$

where $\omega \in (0, 1)$ is the factor which controls the degree of modalities fusion. Then, we substitute $\mathcal{F}_p^{(t)}$ into Eq. (6) to derive the iterative update formula of $\mathcal{F}'_v^{(t)}$:

$$\mathcal{F}'_v^{(t)} = (\omega^2 A)^t \mathcal{F}'_v^{(0)} + (1 - \omega) \sum_{i=0}^{t-1} (\omega^2 A)^i (\omega \mathcal{Z} \mathcal{F}_p^{(0)} + \mathcal{F}'_v^{(0)}), \quad (7)$$

where A denotes $\mathcal{Z} \text{Norm}_1(\mathcal{Z})^\top$. Intuitively, the moment-specific regions of visual features can be fully activated by the guidance of textual features after multiple iterations.

Moreover, to avoid the potential issue of unexpected gradient and high computation cost, we use an approximate inference function based on Neumann Series [25] when $t \rightarrow \infty$:

$$\mathcal{F}'_v^{(\infty)} = (1 - \omega)(I - \omega^2 A)^{-1}(\omega \mathcal{Z} \mathcal{F}_p^{(0)} + \mathcal{F}'_v^{(0)}). \quad (8)$$

In this manner, the model realizes a synergistic temporal and inter-modality relation integration and generates a more comprehensive visual representation \mathcal{F}_v^{new} , i.e., $\mathcal{F}'_v^{(\infty)}$ in Eq. (8).

Global Knowledge Accumulation. As illustrated in Fig. 1, Highlight Detection prioritizes global information of videos. QD-DETR [26] uses a saliency token to capture general information. However, the input-agonist design might cause the inferior perception of the text-related intervals due to the non-referential search area. To mitigate the concern, we propose to use the moment-aware feature as intermediate guidance to accumulate the global knowledge of a video. Specifically, we derive the most relevant snippet \mathcal{F}'_m by measuring the similarity between the moment-wise \mathcal{F}_m and phrase-wise embeddings \mathcal{F}_p . Then, a stack of transformer encoder layers [41] are utilized to excavate the correlation between \mathcal{F}'_m and \mathcal{F}_v^{new} . The overall process is:

$$\mathcal{F}_v^g, \mathcal{F}_v^l = \text{Encoder}(\text{Concat}[\mathcal{F}'_m, \mathcal{F}_v^{new}]). \quad (9)$$

Consequently, the semantic snippet is obliged to focus on the referred moment and suppress the non-target response, which eventually produces the video-wise feature $\mathcal{F}_v^g \in \mathbb{R}^{1 \times D}$. In addition, $\mathcal{F}_v^l \in \mathbb{R}^{L \times D}$ is greatly enriched by the supplement of global information.

3.3. Multi-Aspect Contrastive Learning

As discussed in Sec. 3.2, CIM can better accomplish local relation enhancement in temporal and inter-modality as well as global knowledge accumulation of a video. It is anticipated that the explicit supervision of each objective will further consolidate the effectiveness. To this end, we introduce multi-aspect contrastive learning, which is in two folds:

Clip-Text Alignment. This loss bridges the semantic gap between the textual expression and the clip-level features, which further improves the quality of local relation modeling. Specifically, we first average \mathcal{F}_t to get the sentence-level textual embedding $\mathcal{F}'_t \in \mathbb{R}^{1 \times D}$ and then measure the relevance with clip-level visual representation \mathcal{F}_v^{new} :

$$S_{ct} = \frac{\mathcal{F}_v^{new} \cdot \mathcal{F}'_t^\top}{\|\mathcal{F}_v^{new}\| \cdot \|\mathcal{F}'_t\|}. \quad (10)$$

Finally, we compute the contrastive loss by matrix multiplication:

$$\mathcal{L}_{cta} = -\text{LogSoftmax}(S_{ct}) \cdot G_{ct}, \quad (11)$$

where G_{ct} is annotated to 1 for relevant clips and 0 for others.

Video-Linguist Discrimination. It aims at constructing the fine-grained multi-modal joint space where video-level visual feature $\{\mathcal{F}_{v(i)}^g\}_{i=1}^B$ closens relevant sentence-level textual representation $\{\mathcal{F}'_{t(i)}\}_{i=1}^B$ while distances unrelated ones within a batch B . Similar to [31], the whole process can be formulated as:

$$\mathcal{L}_{vld} = -\sum_{i=1}^B \text{Log} \frac{\exp(\mathcal{F}_{v(i)}^g \cdot \mathcal{F}'_{t(i)}^\top)}{\sum_{j=1}^B \exp(\mathcal{F}_{v(j)}^g \cdot \mathcal{F}'_{t(j)}^\top)}. \quad (12)$$

3.4. Prediction Heads and Loss Function

Multi-Task Prediction Heads. As depicted in Fig. 2, there are two simple heads built on top of the Comprehensive Integration Module for Moment Retrieval and Highlight Detection respectively. Similar to [15, 18, 26], Moment Retrieval Head comprises a standard transformer decoder where we leverage \mathcal{F}_t as the query to generate a series of moment spans P_m . Highlight Detection Head consists of two groups of single fully-connected layer for linear projection. Accordingly, we get the prediction saliency scores $P_s \in \mathbb{R}^{L \times 1}$:

$$P_s = \frac{\mathcal{F}_v^g w_g^\top \cdot \mathcal{F}_v^l w_l^\top}{\sqrt{d}}, \quad (13)$$

where w_g and $w_l \in \mathbb{R}^{d \times D}$ are learnable weights of two Layers.

Total Loss. We supervise our framework by four groups of training objective functions. For MR, $L1$ loss and $GIoU$ loss are adopted to measure the disparity between GT moment G_m and prediction spans P_m :

$$\mathcal{L}_{MR} = \lambda_{gIoU} \mathcal{L}_{gIoU}(P_m, G_m) + \lambda_{L1} \mathcal{L}_{L1}(P_m, G_m). \quad (14)$$

Moreover, the loss functions for HD consist of margin ranking loss \mathcal{L}_{margin} and rank-aware loss \mathcal{L}_{rank} following [26]. Both losses work in tandem to ensure the predicted saliency scores P_s conform to the ground truth scores G_s :

$$\mathcal{L}_{HD} = \lambda_{HD} [\mathcal{L}_{margin}(P_s, G_s) + \mathcal{L}_{rank}(P_s, G_s)] \quad (15)$$

Inspired by [5, 26], we involve hard samples into training process for diversifying the formulations of local and global relationships of different video-text pairs. Briefly, we categorize the lowest relevance between video and text as hard samples and suppress their saliency scores P_s^{hard} during training:

$$\mathcal{L}_{hard} = -\lambda_{hard} \text{Log}(1 - P_s^{hard}) \quad (16)$$

In addition, the objective of multi-aspect contrastive learning promotes semantic associations between text descriptions and visual contents of multi-granularity:

$$\mathcal{L}_{con} = \lambda_{cta} \mathcal{L}_{cta} + \lambda_{vld} \mathcal{L}_{vld}. \quad (17)$$

Method	MR					HD	
	R1		mAP			\geq Very Good	
	@0.5	@0.7	@0.5	@0.75	Avg.	mAP	HIT@1
M-DETR [18]	52.89	33.02	54.82	29.40	30.73	35.69	55.60
UMT† [24]	56.23	41.18	53.83	37.01	36.12	38.18	59.99
UniVTG [21]	58.86	40.86	57.60	35.59	35.47	38.20	60.96
MH-DETR [47]	60.05	42.28	60.75	38.13	38.38	38.22	60.51
QD-DETR† [26]	63.06	45.10	63.04	40.1	40.19	39.04	62.87
EaTR [15]	61.36	45.79	61.86	41.91	41.74	37.15	58.65
UVCOM	63.55	47.47	63.37	42.67	43.18	39.74	64.20
UVCOM †	63.81	48.70	64.47	44.01	43.27	39.79	64.79
<i>With ASR Captions Pretrain</i>							
M-DETR [18]	59.78	40.33	60.51	35.36	36.14	37.43	60.17
UMT [24]	60.83	43.26	57.33	39.12	38.08	39.12	62.39
QD-DETR [26]	64.10	46.10	64.30	40.50	40.62	38.52	62.27
UVCOM	64.53	48.31	64.78	43.65	43.80	39.98	65.58

Table 1. **Jointly MR and HD results on QVHighlights test split.** † indicates training with audio modality. *With ASR Caption Pretrain* denotes models pretrained on ASR captions [18].

Generally, the total loss is expressed as:

$$\mathcal{L}_{total} = \mathcal{L}_{HD} + \mathcal{L}_{MR} + \mathcal{L}_{hard} + \mathcal{L}_{con}. \quad (18)$$

The λ above are hyper-parameters for balancing the losses.

4. Experiments

4.1. Datasets and Evaluation Metrics

Datasets. We evaluate our model on five prevalent MR/HD benchmarks: QVHighlights [18], Charades-STA [7], TaCoS [32], TVSum [37] and YouTube Highlights [38]. Due to the space limitation, the details of each datasets are included in the Appendix B.1.

Metrics. Following [2, 18, 24], we measure the performance of our model by the same criteria for QVhighlights, Charades-STA, TACoS, YouTube Highlights and TVSum. For descriptions of the metrics corresponding to datasets, please see the Appendix B.2.

4.2. Implementation Details

Pre-extracted Features. For a fair comparison, we take the same features of video, text and audio from corresponding pretrained feature extractors, *e.g.*, SlowFast [6], CLIP [31], PANN [16]. For more details please refer to Appendix B.3.

Training Settings. Our model is trained with AdamW optimizer where the learning rate is 1×10^{-4} and weight decay is 1×10^{-4} by default. The encoder of Global Knowledge Accumulation and the decoder of Moment Retrieval Head compose of three layers of transformer blocks. The coefficients for losses are set to $\lambda_{cta} = 0.5$, $\lambda_{hard} = 1$, $\lambda_{vld} =$

Method	Charades-STA		TACoS	
	R1@0.5	R1@0.7	R1@0.5	R1@0.7
2D TAN [56]	46.02	27.50	27.99	12.92
VSLNet [54]	42.69	24.14	23.54	13.15
M-DETR [18]	53.63	31.37	24.67	11.97
QD-DETR [26]	57.31	32.55	–	–
UniVTG [21]	58.01	35.65	34.97	17.35
UVCOM	59.25	36.64	36.39	23.32

Table 2. **MR results on Charades-STA test split and TACoS test split.** The pre-extracted features are from SlowFast [6] and CLIP [31].

0.5, $\lambda_{HD} = 1$, $\lambda_{gIoU} = 1$, $\lambda_{L1} = 10$ in default. Due to space limitations, please see Appendix B.4 for more training details.

4.3. Main Result

QVHighlights. We compare our method to previous methods on QVHighlights in Tab. 1. Benefiting from the comprehensive understanding of the video, our UVCOM achieves new state-of-the-art performance on different settings and shows a significant margin across all metrics. Specifically, our approach outperforms EaTR [15] by 2.25% on the average of all metrics. Incorporating with video and audio modality, UVCOM yields a clear improvement of 3.6% in R1@0.7, 4% in mAP@0.75 for MR and 2% in HID@1 for HD compared to QD-DETR [26]. Furthermore, with ASR caption pretraining, UVCOM achieves the greatest performance on more stringent metrics, *e.g.*, 43.8% in Avg. mAP for MR and 39.98% in Avg. mAP for HD, demonstrating the effectiveness of our method.

Charades-STA & TACoS. In order to evaluate the performance of our method in precise moment localization, we report the results on Charades-STA and TACoS benchmarks. As depicted in Tab. 2, UVCOM outperforms QD-DETR [26] by about 4% R1@0.7 using SlowFast and CLIP features in Charades-STA dataset while boosts 6% R1@0.7 than UniVTG [21] in TaCoS. It is worth noting that we also validate our model surpasses the existing SOTA methods using VGG features (see in Appendix C.1).

YouTube Highlights & TVSum. For Video Highlight Detection, we conduct experiments on TVSum and YouTube Highlights. Considering the fact that the scale and scoring criteria of TVSum is small and inconsistent, our method gains incoherently among domains. However, in Tab. 4, it still boost an improvement of 1.3% in Avg. mAP compared with the SOTA methods. As shown in Tab. 3, our method achieves 76.4% and 77.4% in Avg. mAP without audio source under different settings. Note that the features used in UniVTG [21] and UMT [24] on YouTube Highlights are different. Therefore, we follow the same protocol of each for a fair comparison.

Method	Dog	Gym	Par.	Ska.	Ski.	Sur.	Avg.
GIFs [11]	30.8	33.5	54.0	55.4	32.8	54.1	46.4
LSVM [38]	60.0	41.0	61.0	62.0	36.0	61.0	53.6
LIM-S [45]	57.9	41.7	67.0	57.8	48.6	65.1	56.4
SL-Module [46]	70.8	53.2	77.2	72.5	66.1	76.2	69.3
MINI-Net† [13]	58.2	61.7	70.2	72.2	58.7	65.1	64.4
TCG† [49]	55.4	62.7	70.9	69.1	60.1	59.8	63.0
Joint-VA† [1]	64.5	71.9	80.8	62.0	73.2	78.3	71.8
UMT† [24]	65.9	75.2	81.6	71.8	72.3	82.7	74.9
UniVTG [21]	71.8	76.5	73.9	73.3	73.2	82.2	75.2
UVCOM ¹	73.8	77.1	75.7	75.3	74.0	82.7	76.4
UVCOM ²	66.5	77.4	82.8	78.7	74.2	84.6	77.4

Table 3. **HD results of mAP on YouTube HL.** † denotes using audio modality. 1 and 2 indicate using the same visual and textual features of UniVTG and UMT.

CIM	MCL	MR			HD	
		R1 @0.5	R1 @0.7	mAP Avg.	mAP	HIT@1
		61.55	44.84	40.08	37.10	62.0
✓		62.84	48.77	43.6	39.33	62.97
	✓	60.77	44.06	40.48	38.81	62.06
✓	✓	65.10	51.81	45.79	40.03	63.29

Table 5. **Effectiveness of the proposed modules.**

Method	MR			HD	
	R1 @0.5	R1 @0.7	mAP Avg.	mAP	HIT@1
Average	63.48	49.87	44.10	39.81	63.16
K-Means	62.58	48.39	43.13	39.47	62.26
EM-Att	64.32	50.26	44.49	39.82	64.0
EM-Att†	65.10	51.81	45.79	40.03	63.29

Table 7. **Impact of various aggregation methods.** † indicates the EM Attention module with RBF kernel.

4.4. Ablation Study

In this section, we conduct a series of analysis experiments on the val split of QVHighlights benchmark and train the model from scratch without audio modality.

Component Analysis. We first verify the effectiveness of the proposed Comprehensive Integration Module (CIM) and Multi-Aspect Contrastive Learning (MCL). As illustrated in Tab. 5, both of them brings improvement and their combination contributes to better performance *i.e.*, +5.71% in Avg. mAP, which demonstrates the effectiveness of the comprehensive understanding. To further investigate the validity of three modules involved in CIM, we provide additional experiments on Dual Branches Intra-Modality Aggregation (DBIA), Local Relation Perception (LRP) and Global Knowledge Accumulation (GKA). As shown in Tab. 6, since GKA facilitate the understanding of global context, the ablation of it leads to inferior per-

Method	VT	VU	GA	MS	PK	PR	FM	BK	BT	DS	Avg.
sLSTM [55]	41.1	46.2	46.3	47.7	44.8	46.1	45.2	40.6	47.1	45.5	45.1
LIM-S [45]	55.9	42.9	61.2	54.0	60.4	47.5	43.2	66.3	69.1	62.6	56.3
Trailer [42]	61.3	54.6	65.7	60.8	59.1	70.1	58.2	64.7	65.6	68.1	62.8
SL-Module [46]	86.5	68.7	74.9	86.2	79.0	63.2	58.9	72.6	78.9	64.0	73.3
MINI-Net† [13]	80.6	68.3	78.2	81.8	78.1	65.8	57.8	75.0	80.2	65.5	73.2
TCG† [49]	85.0	71.4	81.9	78.6	80.2	75.5	71.6	77.3	78.6	68.1	76.8
Joint-VA† [1]	83.7	57.3	78.5	86.1	80.1	69.2	70.0	73.0	97.4	67.5	76.3
UniVTG [21]	83.9	85.1	<u>89.0</u>	80.1	84.6	81.4	70.9	<u>91.7</u>	73.5	69.3	81.0
UMT† [24]	87.5	81.5	88.2	78.8	81.5	87.0	76.0	86.9	84.4	79.6	83.1
QD-DETR [26]	88.2	<u>87.4</u>	85.6	85.0	<u>85.8</u>	86.9	<u>76.4</u>	91.3	<u>89.2</u>	<u>73.7</u>	<u>85.0</u>
UVCOM	<u>87.6</u>	91.6	91.4	86.7	86.9	<u>86.9</u>	76.9	92.3	87.4	<u>75.6</u>	86.3

Table 4. **HD results of Top-5 mAP on TVSum.** † denotes using audio modality. The 2-nd performance values are highlighted by underline.

DBIA	LRP	GKA	MR			HD	
			R1 @0.5	R1 @0.7	mAP Avg.	mAP	HIT@1
			60.77	44.06	40.48	38.81	62.06
		✓	62.32	46.71	41.03	38.73	62.58
	✓		62.06	46.45	41.42	38.57	62.45
✓		✓	63.74	49.16	43.45	39.54	64.26
✓	✓		64.71	50.0	43.69	39.69	63.16
	✓	✓	64.84	50.0	44.02	39.58	64.13
✓	✓	✓	65.10	51.81	45.79	40.03	63.29

Table 6. **Effects of the components designed of proposed CIM module.**

Method	MR			HD	
	R1 @0.5	R1 @0.7	mAP Avg.	mAP	HIT@1
Cross Attention	63.03	49.87	43.79	39.63	63.94
BMRW	65.10	51.81	45.79	40.03	63.29

Table 8. **Comparison of different modality interaction strategies.**

formance on HD, *i.e.*, -1.1% in HIT@1. Moreover, LRP brings a clear improvement of +2.34% in Avg. mAP on MR, proving the enhancement on locality perception.

Aggregation Method. We study the impacts on various aggregation methods utilized in DBIA module. As illustrated in Tab. 7, we believe the superiority of our RBF kernel based EM-Attention derives from two aspects: 1) Compared with “Average” and K-Means, our method enhances the desired moment representation while suppresses noises. 2) RBF kernel maps features into a high-dimensional latent space while modeling the relationship within it, which is beneficial for the subsequent aggregation.

Modality Interaction Strategy. We investigate the effects of different modality interaction strategies in Local Relation Perception. As shown in Tab. 8, replacing BMRW by cross attention mechanism results in 2% performance degradation, which demonstrates the effectiveness of BMRW. Furthermore, we provide visualization of fea-

Query: Underwater views of whale sharks and people swimming with them

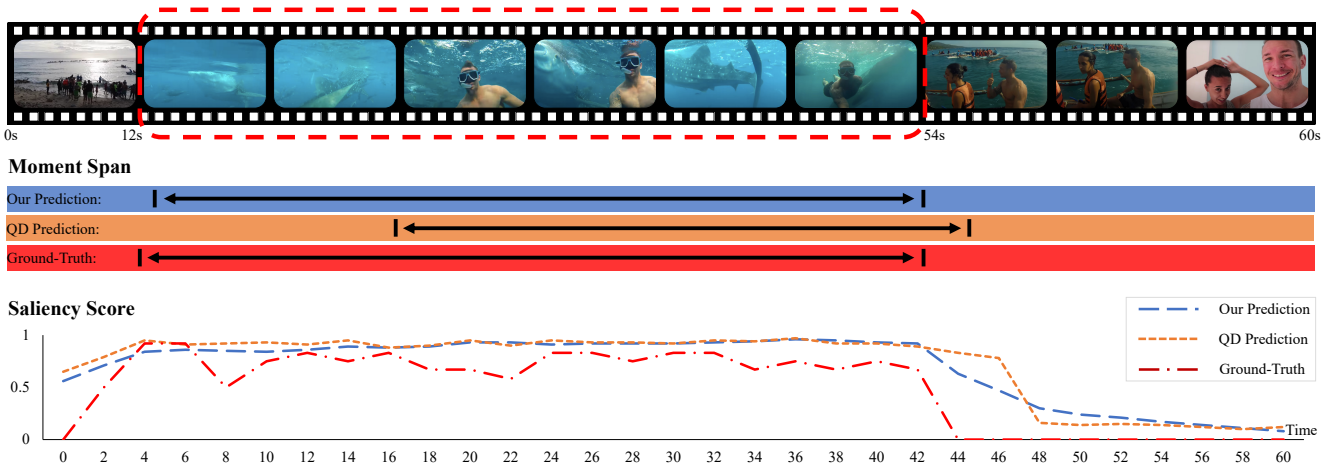


Figure 4. **Visullization comparison on MR and HD.** QD indicates previous state-of-the-art method QD-DETR [26]

Query: The old statues have butterflies on them

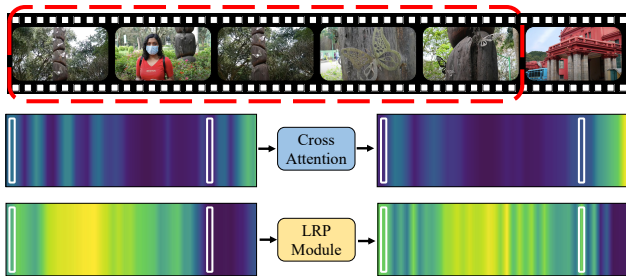


Figure 5. **Illustration of different modality interaction strategies.** The red bounding box indicates the relevant interval and the white bounding box denotes the start and end clips.

tures to prove the rationality of LRP. It can be seen in Fig. 5 that the utilization of cross-attentive mechanism leads to the emergence of attention drift. In contrast, through iterative multi-modal learning in shared space, BMRW mitigates the issue, thereby facilitating more precise localization. Moreover, LRP achieves the local relation perception evidenced by clearer strip-like attention patterns in Fig. 5.

Grounding Consistency. Benefiting from the task-specific design, our method yields greater consistency in the joint solution of MR and HD. To quantify the performance coherence, on one hand, we count the videos with accurate highlight-ness estimation ($mAP_{HD} > 0.8$) and calculate MR mAP for those videos as shown in Fig. 6 (a). On the other hand, we measure the HD mAP and quantities of videos with precise moment spans ($mAP_{MR} > 0.8$) as shown in Fig. 6 (b). The results demonstrate that UVCOM effectively bridges the gap between two tasks for which our method is superior on all statistics, *i.e.*, MR and HD precision as well as quantity.

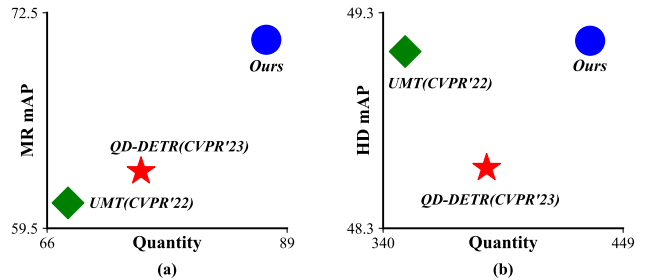


Figure 6. **Illustration of grounding consistency of MR and HD.** (a) indicates the videos collected by $mAP_{HD} > 0.8$. (b) indicates the videos collected by $mAP_{MR} > 0.8$.

4.5. Qualitative Results

As shown in Fig. 4, The local-global enhancement and comprehensive understanding allows our method to accurately model the saliency distribution and localize timestamps of the moment precisely. Comparatively, without the explicit association of characteristics of two tasks, QD-DETR [26] struggles to handle simultaneously in complex scenarios.

5. Conclusion

In light of the different emphasis on MR and HD, we propose a unified video comprehension framework called UVCOM under the guidance of design principles to effectively bridge the gap between two tasks. By performing progressive intra and inter-modality interaction across multi-granularity, UVCOM achieves locality perception of temporal and multi-modal relationship as well as global knowledge accumulation of the entire video. Moreover, we introduce multi-aspect contrastive learning to provide the explicit supervision of above two objectives. Extensive studies validate our model’s comprehensive understanding of

videos and show our UVCOM remarkably outperforms the existing state-of-the-art methods.

Limitations. Our UVCOM has achieved comprehensive understanding of the untrimmed video and superior performance. However, there are some potential limitations, *e.g.*, unable to process auditory descriptions well. Since we just use a simple way to handle audio features instead of specific design, we think that the explicit design for audio features is an interesting future direction.

References

- [1] Taivanbat Badamdorj, Mrigank Rochan, Yang Wang, and Li Cheng. Joint visual and audio learning for video highlight detection. In *ICCV*, pages 8107–8117, 2021. 1, 2, 7
- [2] Nicolas Carion, Francisco Massa, Gabriel Synnaeve, Nicolas Usunier, Alexander Kirillov, and Sergey Zagoruyko. End-to-end object detection with transformers. In *ECCV*, pages 213–229, 2020. 2, 6
- [3] Joao Carreira and Andrew Zisserman. Quo vadis, action recognition? a new model and the kinetics dataset. In *CVPR*, pages 6299–6308, 2017. 3, 1
- [4] Shaoxiang Chen and Yu-Gang Jiang. Semantic proposal for activity localization in videos via sentence query. In *AAAI*, pages 8199–8206, 2019. 1
- [5] Qi Dong, Shaogang Gong, and Xiatian Zhu. Class rectification hard mining for imbalanced deep learning. In *ICCV*, pages 1851–1860, 2017. 5
- [6] Christoph Feichtenhofer, Haoqi Fan, Jitendra Malik, and Kaiming He. Slowfast networks for video recognition. In *ICCV*, pages 6201–6210, 2019. 3, 6, 1
- [7] Jiyang Gao, Chen Sun, Zhenheng Yang, and Ram Nevatia. Tall: Temporal activity localization via language query. In *ICCV*, pages 5267–5275, 2017. 6, 2
- [8] Jiyang Gao, Chen Sun, Zhenheng Yang, and Ram Nevatia. TALL: temporal activity localization via language query. In *ICCV*, pages 5277–5285, 2017. 1, 2
- [9] Jialin Gao, Xin Sun, Mengmeng Xu, Xi Zhou, and Bernard Ghanem. Relation-aware video reading comprehension for temporal language grounding. In *EMNLP*, pages 3978–3988, 2021. 2
- [10] Leo Grady. Random walks for image segmentation. *IEEE Trans. Pattern Anal. Mach. Intell.*, 28(11):1768–1783, 2006. 4
- [11] Michael Gygli, Yale Song, and Liangliang Cao. Video2gif: Automatic generation of animated gifs from video. In *CVPR*, pages 1001–1009, 2016. 1, 2, 7
- [12] Lisa Anne Hendricks, Oliver Wang, Eli Shechtman, Josef Sivic, Trevor Darrell, and Bryan C. Russell. Localizing moments in video with temporal language. In *EMNLP*, pages 1380–1390, 2018. 2
- [13] Fa-Ting Hong, Xuanteng Huang, Weihong Li, and Wei-Shi Zheng. Mini-net: Multiple instance ranking network for video highlight detection. In *ECCV*, pages 345–360, 2020. 7
- [14] Linjiang Huang, Liang Wang, and Hongsheng Li. Weakly supervised temporal action localization via representative snippet knowledge propagation. In *CVPR*, pages 3262–3271, 2022. 3, 4
- [15] Jinhyun Jang, Jungin Park, Jin Kim, Hyeongjun Kwon, and Kwanghoon Sohn. Knowing where to focus: Event-aware transformer for video grounding. *arXiv preprint arXiv: 2308.06947*, 2023. 5, 6
- [16] Qiuqiang Kong, Yin Cao, Turab Iqbal, Yuxuan Wang, Wenwu Wang, and Mark D Plumbley. Panns: Large-scale pretrained audio neural networks for audio pattern recognition. *IEEE ACM Trans. Audio Speech Lang. Process.*, 28: 2880–2894, 2020. 6, 1
- [17] Jie Lei, Licheng Yu, Tamara L. Berg, and Mohit Bansal. TVR: A large-scale dataset for video-subtitle moment retrieval. In *ECCV*, pages 447–463, 2020. 2
- [18] Jie Lei, Tamara L. Berg, and Mohit Bansal. Qvhighlights: Detecting moments and highlights in videos via natural language queries. *arXiv preprint arXiv: 2107.09609*, 2021. 1, 2, 3, 4, 5, 6
- [19] Kun Li, Dan Guo, and Meng Wang. Proposal-free video grounding with contextual pyramid network. In *AAAI*, pages 1902–1910, 2021. 2
- [20] Xia Li, Zhisheng Zhong, Jianlong Wu, Yibo Yang, Zhouchen Lin, and Hong Liu. Expectation-maximization attention networks for semantic segmentation. In *ICCV*, pages 9166–9175, 2019. 3
- [21] Kevin Qinghong Lin, Pengchuan Zhang, Joya Chen, Shraman Pramanick, Difei Gao, Alex Jinpeng Wang, Rui Yan, and Mike Zheng Shou. Univgt: Towards unified video-language temporal grounding. *arXiv preprint arXiv: 2307.16715*, 2023. 2, 3, 6, 7
- [22] Meng Liu, Xiang Wang, Liqiang Nie, Xiangnan He, Baoquan Chen, and Tat-Seng Chua. Attentive moment retrieval in videos. In *SIGIR*, pages 15–24, 2018. 2
- [23] Meng Liu, Xiang Wang, Liqiang Nie, Qi Tian, Baoquan Chen, and Tat-Seng Chua. Cross-modal moment localization in videos. In *ACM MM*, pages 843–851, 2018. 1
- [24] Ye Liu, Siyuan Li, Yang Wu, Chang Wen Chen, Ying Shan, and Xiaohu Qie. UMT: unified multi-modal transformers for joint video moment retrieval and highlight detection. In *CVPR*, pages 3032–3041, 2022. 1, 2, 3, 4, 6, 7
- [25] Carl D Meyer and Ian Stewart. *Matrix analysis and applied linear algebra*. SIAM, 2023. 5, 1
- [26] WonJun Moon, Sangeek Hyun, Sanguk Park, Dongchan Park, and Jae-Pil Heo. Query - dependent video representation for moment retrieval and highlight detection. In *CVPR*, 2023. 1, 2, 3, 4, 5, 6, 7, 8
- [27] Jonghwan Mun, Minsu Cho, and Bohyung Han. Local-global video-text interactions for temporal grounding. In *CVPR*, pages 10807–10816, 2020. 2
- [28] Giannis Nikolentzos and Michalis Vazirgiannis. Random walk graph neural networks. In *NeurIPS*, 2020. 4
- [29] Cristian Rodriguez Opazo, Edison Marrese-Taylor, Fateh Sadat Saleh, Hongdong Li, and Stephen Gould. Proposal-free temporal moment localization of a natural-language query in video using guided attention. In *WACV*, pages 2453–2462, 2020. 2

- [30] Jeffrey Pennington, Richard Socher, and Christopher D Manning. Glove: Global vectors for word representation. In *EMNLP*, pages 1532–1543, 2014. [1](#)
- [31] Alec Radford, Jong Wook Kim, Chris Hallacy, Aditya Ramesh, Gabriel Goh, Sandhini Agarwal, Girish Sastry, Amanda Askell, Pamela Mishkin, Jack Clark, Gretchen Krueger, and Ilya Sutskever. Learning transferable visual models from natural language supervision. In *ICML*, pages 8748–8763, 2021. [3](#), [5](#), [6](#), [1](#)
- [32] Michaela Regneri, Marcus Rohrbach, Dominikus Wetzel, Stefan Thater, Bernt Schiele, and Manfred Pinkal. Grounding action descriptions in videos. *Trans. Assoc. Comput. Linguistics*, 1:25–36, 2013. [2](#), [6](#)
- [33] Sylvia Richardson and Peter J Green. On bayesian analysis of mixtures with an unknown number of components (with discussion). *Journal of the Royal Statistical Society Series B: Statistical Methodology*, 59(4):731–792, 1997. [3](#)
- [34] Mrigank Rochan, Mahesh Kumar Krishna Reddy, Linwei Ye, and Yang Wang. Adaptive video highlight detection by learning from user history. In *ECCV*, pages 261–278, 2020. [2](#)
- [35] Erica K Shimomoto, Edison Marrese-Taylor, Hiroya Takamura, Ichiro Kobayashi, Hideki Nakayama, and Yusuke Miyao. Towards parameter-efficient integration of pre-trained language models in temporal video grounding. *arXiv preprint arXiv:2209.13359*, 2022. [1](#)
- [36] Karen Simonyan and Andrew Zisserman. Very deep convolutional networks for large-scale image recognition. In *ICLR*, 2015. [1](#)
- [37] Yale Song, Jordi Vallmitjana, Amanda Stent, and Alejandro Jaimes. Tvsum: Summarizing web videos using titles. In *CVPR*, pages 5179–5187, 2015. [6](#)
- [38] Min Sun, Ali Farhadi, and Steve Seitz. Ranking domain-specific highlights by analyzing edited videos. In *ECCV*, pages 787–802, 2014. [6](#), [7](#)
- [39] Xin Sun, Xuan Wang, Jialin Gao, Qiong Liu, and Xi Zhou. You need to read again: Multi-granularity perception network for moment retrieval in videos. In *SIGIR*, pages 1022–1032, 2022. [2](#)
- [40] Haoyu Tang, Jihua Zhu, Meng Liu, Zan Gao, and Zhiyong Cheng. Frame-wise cross-modal matching for video moment retrieval. *TMM*, 24:1338–1349, 2022. [2](#)
- [41] Ashish Vaswani, Noam Shazeer, Niki Parmar, Jakob Uszkoreit, Llion Jones, Aidan N Gomez, Łukasz Kaiser, and Illia Polosukhin. Attention is all you need. *NeurIPS*, 30, 2017. [5](#)
- [42] Lezi Wang, Dong Liu, Rohit Puri, and Dimitris N Metaxas. Learning trailer moments in full-length movies with co-contrastive attention. In *ECCV*, pages 300–316, 2020. [7](#)
- [43] Weining Wang, Yan Huang, and Liang Wang. Language-driven temporal activity localization: A semantic matching reinforcement learning model. In *CVPR*, pages 334–343, 2019. [1](#)
- [44] Shaoning Xiao, Long Chen, Songyang Zhang, Wei Ji, Jian Shao, Lu Ye, and Jun Xiao. Boundary proposal network for two-stage natural language video localization. In *AAAI*, pages 2986–2994, 2021. [2](#)
- [45] Bo Xiong, Yannis Kalantidis, Deepti Ghadiyaram, and Kristen Grauman. Less is more: Learning highlight detection from video duration. In *CVPR*, pages 1258–1267, 2019. [1](#), [2](#), [7](#)
- [46] Minghao Xu, Hang Wang, Bingbing Ni, Riheng Zhu, Zhenbang Sun, and Changhu Wang. Cross-category video highlight detection via set-based learning. In *ICCV*, pages 7950–7959, 2021. [7](#)
- [47] Yifang Xu, Yunzhuo Sun, Yang Li, Yilei Shi, Xiaoxiang Zhu, and Sidan Du. Mh-detr: Video moment and highlight detection with cross-modal transformer. *arXiv preprint arXiv:2305.00355*, 2023. [6](#)
- [48] Ting Yao, Tao Mei, and Yong Rui. Highlight detection with pairwise deep ranking for first-person video summarization. In *CVPR*, pages 982–990, 2016. [1](#), [2](#)
- [49] Qinghao Ye, Xiyue Shen, Yuan Gao, Zirui Wang, Qi Bi, Ping Li, and Guang Yang. Temporal cue guided video highlight detection with low-rank audio-visual fusion. In *ICCV*, pages 7950–7959, 2021. [7](#)
- [50] Youngjae Yu, Sangho Lee, Joonil Na, Jaeyun Kang, and Gunhee Kim. A deep ranking model for spatio-temporal highlight detection from a 360 video. In *AAAI*, pages 7525–7533, 2018. [1](#), [2](#)
- [51] Yitian Yuan, Tao Mei, and Wenwu Zhu. To find where you talk: Temporal sentence localization in video with attention based location regression. In *AAAI*, pages 9159–9166, 2019. [2](#)
- [52] Yawen Zeng, Ning Han, Keyu Pan, and Qin Jin. Temporally language grounding with multi-modal multi-prompt tuning. *TMM*, 2023. [1](#)
- [53] Da Zhang, Xiyang Dai, Xin Wang, Yuan-Fang Wang, and Larry S. Davis. MAN: moment alignment network for natural language moment retrieval via iterative graph adjustment. In *CVPR*, pages 1247–1257, 2019. [1](#), [2](#)
- [54] Hao Zhang, Aixin Sun, Wei Jing, and Joey Tianyi Zhou. Span-based localizing network for natural language video localization. In *ACL*, pages 6543–6554, 2020. [2](#), [6](#)
- [55] Ke Zhang, Wei-Lun Chao, Fei Sha, and Kristen Grauman. Video summarization with long short-term memory. In *ECCV*, pages 766–782, 2016. [7](#)
- [56] Songyang Zhang, Houwen Peng, Jianlong Fu, and Jiebo Luo. Learning 2d temporal adjacent networks for moment localization with natural language. In *AAAI*, pages 12870–12877, 2020. [6](#), [1](#)

Appendix

A. Additional Details about Bidirectional Modality Random Walk Algorithm.

As stated in the manuscript, we propose a Bidirectional Modality Random Walk algorithm (BMRW) to exploit the power of the fine-grained multi-modal interaction. In this section, we provide in-depth illustration on it. First, we define the linguistic feature $\mathcal{F}_p^{(0)}$ and visual feature $\mathcal{F}'_v^{(0)}$ as initial variables at 0-th iteration:

$$\begin{cases} \mathcal{F}_p^{(0)} = \mathcal{F}_p \\ \mathcal{F}'_v^{(0)} = \mathcal{F}'_v \\ \mathcal{Z} = \lambda_z \mathcal{F}'_v^{(0)} (\mathcal{F}_p^{(0)})^\top, \end{cases} \quad (19)$$

where \mathcal{Z} is the affinity between two modalities. Then we propagate the semantics between modalities in two iterative formulas:

$$\begin{cases} \mathcal{F}_p^{(t)} = \omega \text{Norm1}(\mathcal{Z})^\top \mathcal{F}'_v^{(t-1)} + (1 - \omega) \mathcal{F}_p^{(0)} \\ \mathcal{F}'_v^{(t)} = \omega \mathcal{Z} \mathcal{F}_p^{(t)} + (1 - \omega) \mathcal{F}'_v^{(0)}, \quad \omega \in (0, 1). \end{cases} \quad (20)$$

Integrating Eq. (20) we can get:

$$\begin{aligned} \mathcal{F}'_v^{(t)} &= (\omega^2 \text{ZNorm1}(\mathcal{Z})^\top) \mathcal{F}'_v^{(t-1)} \\ &\quad + \omega(1 - \omega) \mathcal{Z} \mathcal{F}_p^{(0)} + (1 - \omega) \mathcal{F}'_v^{(0)} \\ &= (\omega^2 \text{ZNorm1}(\mathcal{Z})^\top) \mathcal{F}'_v^{(t-1)} \\ &\quad + (1 - \omega)(\omega \mathcal{Z} \mathcal{F}_p^{(0)} + \mathcal{F}'_v^{(0)}). \end{aligned} \quad (21)$$

We substitute $\text{ZNorm1}(\mathcal{Z})^\top$ as A and expand Eq. (21) from t -th to 0-th iteration:

$$\mathcal{F}'_v^{(t)} = (\omega^2 A)^t \mathcal{F}'_v^{(0)} + (1 - \omega) \sum_{i=0}^{t-1} (\omega^2 A)^i (\omega \mathcal{Z} \mathcal{F}_p^{(0)} + \mathcal{F}'_v^{(0)}), \quad (22)$$

Considering the potential risk of unexpected gradient or expensive computation cost, we use an approximate optimal solution based on Neumann Series [25]:

$$\lim_{t \rightarrow \infty} \sum_{i=0}^{t-1} (\omega^2 A)^i = (I - \omega^2 A)^{-1}. \quad (23)$$

Accordingly, when $t \rightarrow \infty$ in Eq. (22), the comprehensive visual representation is generated as:

$$\mathcal{F}'_v^{(\infty)} = (1 - \omega)(I - \omega^2 A)^{-1} (\omega \mathcal{Z} \mathcal{F}_p^{(0)} + \mathcal{F}'_v^{(0)}). \quad (24)$$

B. Additional Details on Experiment Settings

B.1. Datasets

QVHighlight is the most popular publicized dataset which consists of over 10,000 videos with human-written free-form text descriptions for moment retrieval and highlight

Method	R1@0.5	R1@0.7
SAP [4]	27.42	13.36
SM-RL [43]	24.36	11.17
MAN [53]	41.24	20.54
2D-TAN [56]	40.94	22.85
QD-DETR [26]	52.77	31.13
UVCOM	54.57	34.13
UMT† [24]	48.31	29.25
QD-DETR† [26]	55.51	34.17
UVCOM†	56.69	34.76

Table 9. **MR results on Charades-STA Test Split.** The pre-extracted features are from VGG, GLOVE Embeddings and PANN. † denotes using audio modality

detection. Charades-STA and TACoS are both for moment retrieval where Charades-STA comprises 16,128 query-moment pairs for indoor activities and TACoS contains 127 annotated videos from cooking scenarios. TVSum and YouTube Highlights cater for highlight detection. Each of which includes 10 domains with 5 videos and 6 domains with 433 videos respectively.

B.2. Metrics

Recall@1 with IoU thresholds 0.5 and 0.7, mean average precision (mAP) with IoU thresholds 0.5 and 0.75 as well as average mAP over 0.5:0.05:0.95 are for MR, while mAP and HIT@1 are used for HD. HIT@1 is computed through the hit ratio of the clip with the highest score. For Charades-STA and TACoS, we report the result of Recall@1 with IoU thresholds 0.5 and 0.7. For YouTube Highlights and TVSum, we follow [24] and adopt the metrics of mAP and Top-5 mAP.

B.3. Feature Representations

The pre-extracted visual and text features from SlowFast [6] and CLIP [31] are used on all datasets. Notably, on Charades-STA and YouTube Highlights, we additionally extract the features from official VGG [36] as well as GLOVE [30] embeddings and commonly used I3D [3], respectively for further comparisons. Besides, we leverage PANN [16] model to encode audio features for experiments with extra audio modality learning.

B.4. Training Details

Elaborate parameter settings for each benchmark are summarized in Tab. 10. For more details, all experiments are implemented in PyTorch with one 24GB RTX3090. The overall aggregation for DBIA is performed in 5 iterations. In addition, the hidden dimension of transformer is 256 for all experiments.

Dataset	Feature	Lr	Epoch	Bs	Lr drop	n_v	n_t	λ_{IoU}	λ_{L1}	λ_{HD}	λ_{hard}	λ_{cta}	λ_{vld}
QVHighlights	SF+C	1e-4	200	32	100	30	5	1	10	1	1	0.5	0.5
Charades-STA	SF+C	1e-4	200	8	80	30	5	1	10	1	1	0.5	0.5
Charades-STA	VGG	1e-4	200	8	-	30	5	1	10	1	1	1.5	0.5
TaCoS	SF+C	1e-4	200	32	100	30	5	1	10	1	1	0.5	0.5
TVSum	I3D	1e-4	2000	4	-	30	5	1	10	1	1	Tab. 15	Tab. 15
YouTubeHL	SF+C	1e-4	2000	4	1000	30	2	-	-	1	1	Tab. 16	Tab. 16
YouTubeHL	I3D	1e-4	2000	4	1000	30	2	-	-	1	1	Tab. 17	Tab. 17

Table 10. **Training details.** We provide elaborate training details on each dataset. Lr denotes learning rate; Bs denotes batch size; Lr drop denotes the drop of learning rate at the specific epoch. n_v and n_t denote the number of Gaussians in DBIA module.

n_v	n_t	MR			HD	
		R1 @0.5	R1 @0.7	mAP Avg.	mAP	HIT@1
20	3	62.58	48.45	42.44	39.58	61.87
25	4	64.45	50.06	42.95	40.0	64.9
25	5	64.26	50.06	43.48	39.51	62.06
30	5	65.10	51.81	45.79	40.03	63.29
30	6	62.19	48.52	43.53	39.9	64.32

Table 11. **Results of different numbers of Gaussian for video and text.**

Iterations	MR			HD	
	R1 @0.5	R1 @0.7	mAP Avg.	mAP	HIT@1
3	63.55	48.52	43.19	40.03	64.26
4	63.48	50.0	44.09	39.77	64.71
5	65.10	51.81	45.79	40.03	63.29
6	62.65	47.94	43.09	39.44	62.77

Table 13. **Results of different iterations of EM Attention.**

C. Additional Experiments

C.1. Result on Charades-STA

We also present comparisons on Charades-STA [7] with existing methods in Tab. 9. As observed, our UVCOM achieve the new state-of-the-art performance under different settings, which further validates the rationality of our design in local perception enhancement for MR.

C.2. Additional Ablation Studies

We conduct additional analysis experiments on the val split of QVHighlights benchmark.

Number of Gaussian. The degree of the intra-modality aggregation is determined by the number of Gaussian. Specifically, we conduct ablation studies on two parameters n_v and n_t where each denotes the number of condense visual and linguistic outputs in Tab. 11. We find that the performance tends to boost as the number of Gaussians in-

λ_{cta}	λ_{vld}	MR			HD	
		R1 @0.5	R1 @0.7	mAP Avg.	mAP	HIT@1
0.3	0.7	63.61	48.19	43.68	39.88	63.68
0.5	1.0	64.84	50.13	44.69	40.02	64.13
0.5	0.5	65.10	51.81	45.79	40.03	63.29
1.5	0.7	64.13	49.81	43.97	39.96	63.48

Table 12. **Results of the different hyper-parameters in Multi-Aspect Contrastive Learning.**

Layer Num.	MR			HD	
	R1 @0.5	R1 @0.7	mAP Avg.	mAP	HIT@1
2	61.74	46.52	41.18	39.81	63.1
3	65.10	51.81	45.79	40.03	63.29
4	63.68	49.61	43.8	39.63	62.65
5	63.55	49.16	43.73	39.56	62.77

Table 14. **Results of different numbers of encoder and decoder layers.**

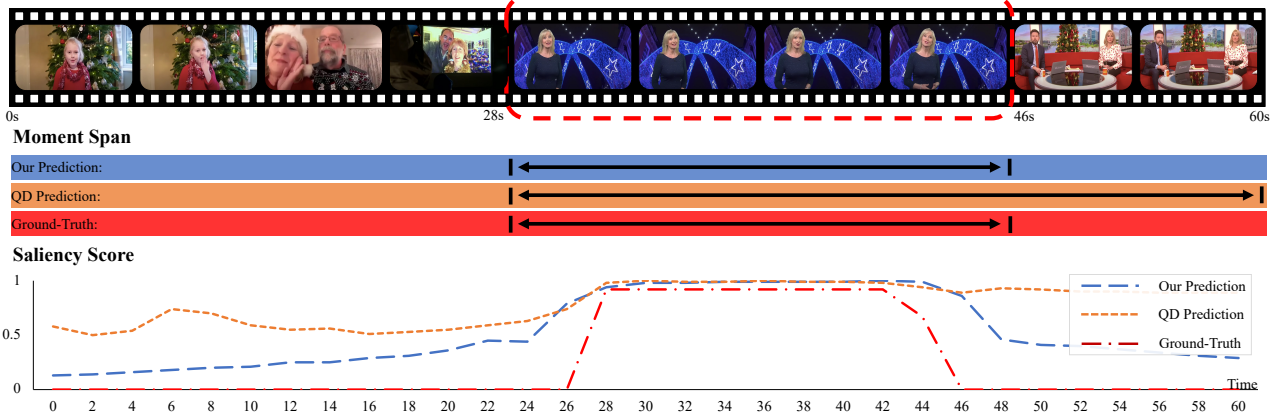
creases for which the smaller one may lead to inefficiency for content clustering in video or text. However, the large value of Gaussians degrades the performance. We assume that the larger one introduces redundancy, which hinders the converge process.

Multi-Aspect Contrastive Learning Coefficients. For multi-aspect contrastive learning, \mathcal{L}_{cta} , \mathcal{L}_{vld} are coefficients for clip-text alignment and video-linguist discrimination loss respectively. We report the ablation results in Tab. 12. As observed, the appropriate setting of coefficient helps decently solidify the local relation modeling and global knowledge integration, thereby facilitating the comprehensive understanding.

Aggregation Iteration. The aggregation iteration controls the quality of multi-grained feature generation, *i.e.*, moment-level and phrase-level features. It can be seen in Tab. 13 that the insufficient or excessive iterations both lead

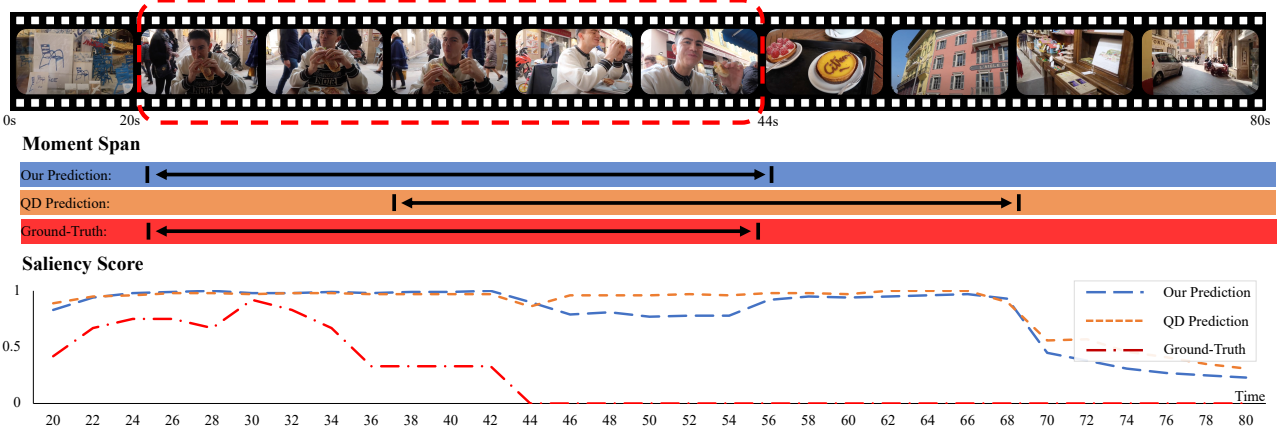
(a)

Query: A woman in a blue dress is speaking in front of a display of blue banners with stars on them



(b)

Query: A man sitting down at a French cafe and enjoying a sandwich there



(c)

Query: A tourist couple get the mango smoothie ball at the Bricklin Cafe in Penang, Malaysia

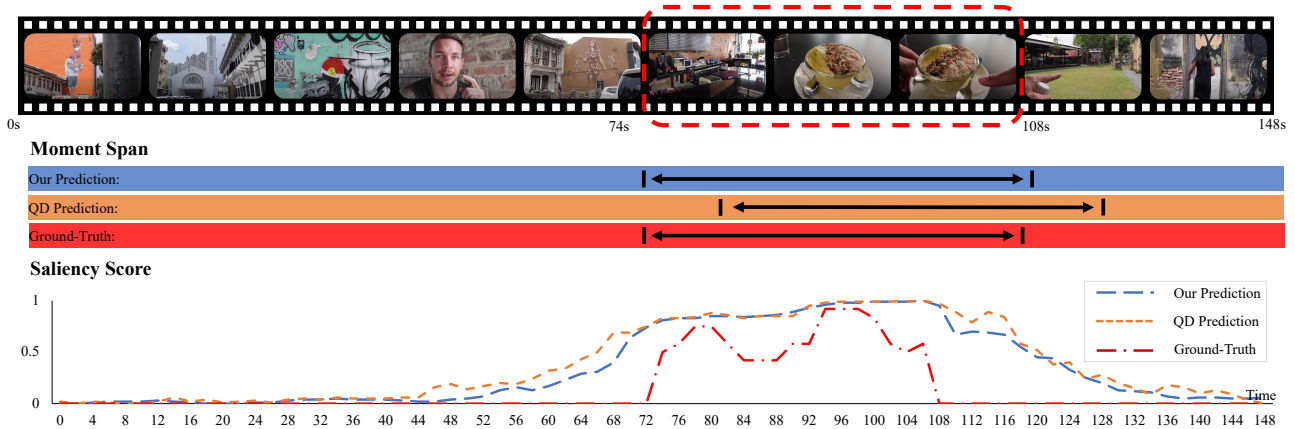
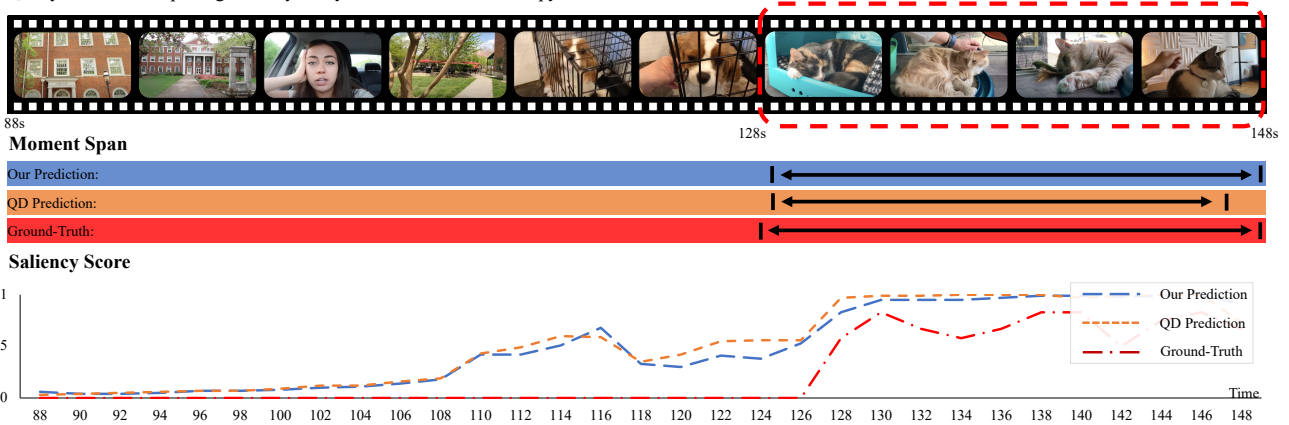


Figure 7. Visualization comparison on MR and HD. QD indicates previous state-of-the-art method QD-DETR [26]

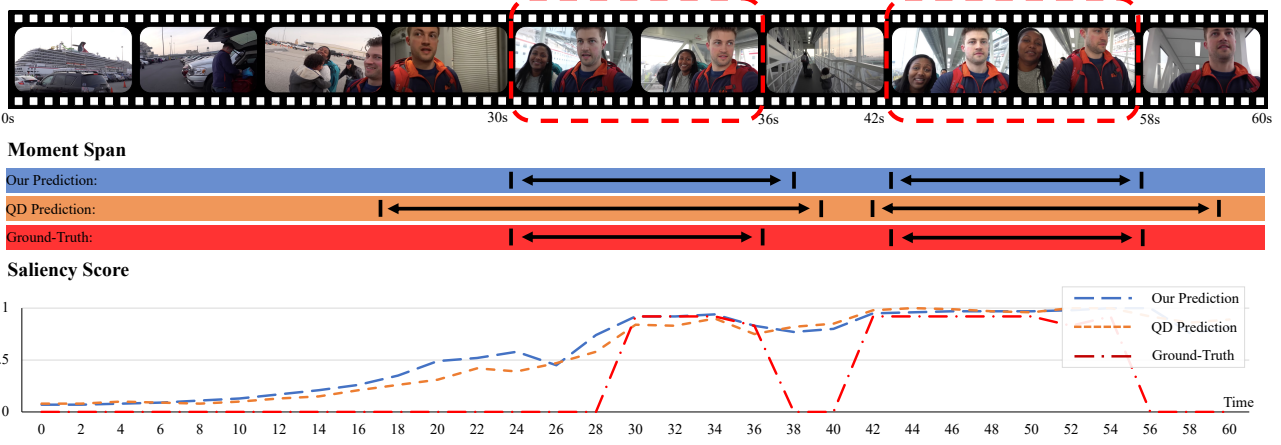
(e)

Query: A woman is petting her very fluffy cat who looks to be sleepy



(f)

Query: Man and woman head through a glass walkway together



(g)

Query: Two girls are comparing the shoes they are wearing together

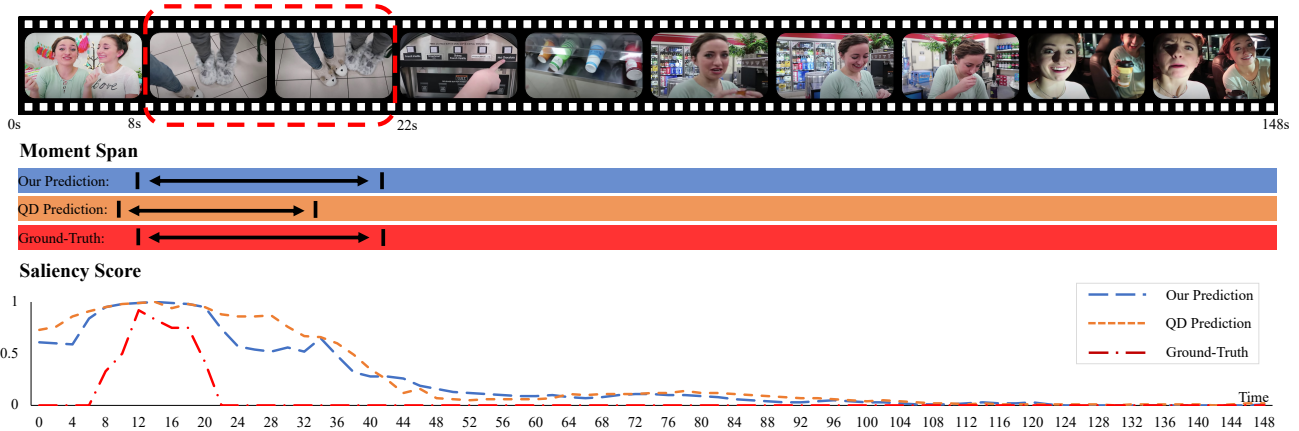


Figure 8. Visualization comparison on MR and HD. QD indicates previous state-of-the-art method QD-DETR [26]

Domain	VT	VU	GA	MS	PK	PR	FM	BK	BT	DS
λ_{cta}	0.4	0.75	0.5	0.1	0.3	1.0	0.25	0.5	1	0.25
λ_{vld}	0.2	0.75	0.5	0.1	0.3	0	0.25	0.5	0	0.25

Table 15. λ_{cta} and λ_{vld} for TVSum.

Domain	Dog	Gym.	Park.	Ska.	Ski.	Surf.
λ_{cta}	0.5	0.8	0	0.5	0	0.5
λ_{vld}	1	0.8	1.5	1	1.5	1

Table 16. λ_{cta} and λ_{vld} for YoutubeHL using SF+C feature.

Domain	Dog	Gym.	Park.	Ska.	Ski.	Surf.
λ_{cta}	0.5	0.8	1.0	0.5	1.0	0.5
λ_{vld}	0.5	0.8	1.5	1	1.5	0.5

Table 17. λ_{cta} and λ_{vld} for YoutubeHL using I3D feature.

to the decreased performance due to the incomplete contextual information fusion or over exaggeration on similar contents.

Layers. To investigate the impact on the different encoder and decoder layers, we provide the performance variation in Tab. 14. The results depict that the increased layers bring significant improvement. However, the performance saturates when the number of layers reaches 5. This can be attributed to the noises accumulation caused by redundant interaction.

C.3. Visualizations.

Fig. 7 and Fig. 8 display additional qualitative comparisons between our UVCOM and a previous state-of-the-art method, which shows our consistent performance on Moment Retrieval and Highlight Detection.